Magnetic Resonance Imaging 122 (2025) 110423

Contents lists available at ScienceDirect

Magnetic Resonance Imaging

journal homepage: www.elsevier.com/locate/mri

Imaging of the renal allograft vasculature without gadolinium contrast: Intraindividual comparison between relaxation-enhanced angiography without contrast and triggering (REACT) and 4D contrast-enhanced MR-angiography

Carsten Gietzen [a,*], Juliana Tristram [a], Jan Paul Janssen [a], Marielle Hummels [b], Johannes Bremm [a], Kenan Kaya [a], Thorsten Gietzen [c], Henry Pennig [d], Roman Gertz [a], Thorsten Persigehl [a], Dirk Stippel [b], Kilian Weiss [e], Lenhard Pennig [a]

[a] Institute for Diagnostic and Interventional Radiology, Faculty of Medicine and University Hospital Cologne, University of Cologne, Cologne, Germany
[b] Department of General, Visceral, Cancer and Transplant Surgery, Faculty of Medicine and University Hospital of Cologne, University of Cologne, Cologne, Germany
[c] Department of Cardiology, Heart Center, Faculty of Medicine and University Hospital Cologne, University of Cologne, Cologne, Germany
[d] Department of Orthopedics and Trauma Surgery, University Hospital Bonn, Bonn, Germany
[e] Philips GmbH, Hamburg, Germany

ARTICLE INFO

Keywords:
Renal allograft vasculature
Transplant renal artery stenosis
Pelvic arteries and veins
Contrast-enhanced magnetic resonance angiography
Relaxation-enhanced angiography without contrast and triggering

ABSTRACT

Background: Complications after kidney transplantation include transplant renal artery stenosis (TRAS), which can be assessed using Doppler ultrasonography, computed tomography angiography, and magnetic resonance angiography (MRA). Contrast-enhanced MRA (CE-MRA) has limitations, including potential allergic reactions, limited use in kidney failure, and uncertain long-term effects of gadolinium retention.
Purpose: To evaluate Relaxation-Enhanced Angiography without Contrast and Triggering (REACT), a novel 3D isotropic flow-independent non-CE-MRA pulse sequence, for imaging of the renal allograft vasculature by performing an intraindividual comparison to 4D CE-MRA at 3Tesla.
Methods: Forty studies of 39 patients were included in this retrospective, single-centre study. Two board-certified radiologists independently evaluated MRA datasets for TRAS and rated their diagnostic confidence and the image quality of pelvic vessels using 5-point Likert scales (5 = excellent). Apparent signal- and contrast-to-noise ratios (aSNR/aCNR) were measured for arterial and venous graft vessels.
Results: REACT (median acquisition time 04:33 min [IQR 3:58–5:20 min]) showed 90.0 % sensitivity and 100.0 % specificity for TRAS in almost perfect agreement ($r = 0.97$) with 4D CE-MRA (03:41 min [3:38–4:46 min], $p = 0.001$) and similar diagnostic confidence (REACT: 4.0 [4.0–4.0] vs. 4D CE-MRA: 4.0 [3.0–4.0], $p = 0.54$). Arterial image quality was comparable (4.0 [3.7–4.4] vs. 4.0 [4.0–4.4], $p = 0.49$) whereas veins yielded higher scores in REACT (3.2 [3.0–3.5] vs. 2.4 [2.0–3.0], $p < 0.001$). Transplant renal artery (mean ± SD; 44.5 ± 18.2 vs. 45.9 ± 21.0, $p = 0.71$; 36.3 ± 15.0 vs. 41.0 ± 20.0, $p = 0.16$) and vein (37.1 ± 19.8 vs. 30.3 ± 15.2, $p = 0.06$; 29.4 ± 17.1 vs. 25.0 ± 14.7, $p = 0.17$) showed no difference in aSNR and aCNR.
Conclusion: REACT provides accurate detection of TRAS with image quality comparable to 4D CE-MRA, offering a risk-free alternative for imaging after renal transplantation.

Abbreviations: AA, abdominal aorta; AV, arterio-venous; CE-MRA, contrast-enhanced magnetic resonance angiography; CIA, common iliac artery; CIV, common iliac vein; CKD, chronic kidney disease; ECG, electrocardiogram; ESRD, end-stage renal disease; EIA, external iliac artery; EIV, external iliac vein; GFR, glomerular filtration rate; IQR, interquartile range; IIA, internal iliac artery; IIV, internal iliac vein; IVC, inferior vena cava; MIP, maximum intensity projection; mDixon, modified Dixon technique; QISS, quiescent-inflow single shot; REACT, relaxation-enhanced angiography without contrast and triggering; SENSE, SENSitivity Encoding; SD, standard deviation; SSFP, steady-state free precession; TRAS, ransplant renal artery stenosis; TA, transplant renal artery; TV, transplant renal vein.

* Corresponding author at: Institute for Diagnostic and Interventional Radiology, Faculty of Medicine and University Hospital Cologne, University of Cologne, Kerpener Straße 62, 50937 Cologne, Germany.
E-mail address: Carsten.gietzen@uk-koeln.de (C. Gietzen).

https://doi.org/10.1016/j.mri.2025.110423
Received 6 March 2025; Received in revised form 13 May 2025; Accepted 16 May 2025
Available online 18 May 2025

1. Introduction

Kidney transplantation is regarded as the optimal treatment in end-stage renal disease (ESRD) [1] with 112.517 procedures performed worldwide in 2023 [2]. However, there is a considerable risk for post-operative complications, including transplant renal artery stenosis (TRAS), which has been reported in up to 25 % of cases [3]. TRAS may lead to symptoms such as arterial hypertension and a decline in renal function [4]. If left undiagnosed or untreated, TRAS has the potential to compromise the renal allograft function [5] and even result in graft failure [6]. In later stages, consequently, the detection of TRAS is pivotal to prevent graft failure. Hence, transplant teams integrate different diagnostic methods, such as color flow Doppler ultrasonography [7], contrast-enhanced magnetic resonance angiography (CE-MRA) [8], computed tomography angiography (CTA), digital subtraction angiography (DSA) [9], and renal biopsy [10] for the follow-up of renal transplant patients [11]. Given its radiation-free and minimal-invasive approach, CE-MRA has been increasingly utilized in recent years. Nonetheless, the use of intravenous contrast administration in CE-MRA has drawbacks such as limited use in patients with kidney failure [11], the potential for nephrogenic systemic fibrosis [12], uncertain long-term effects of gadolinium deposition [13], allergic reactions [14], and potential mistiming of image acquisition [15].

Therefore, various non-CE-MRA techniques have been evaluated for renal graft vessel imaging [16]. Currently, the most widely used non-CE-MRA techniques are balanced steady-state free precession (bSSFP) [17] and quiescent-inflow single shot (QISS)-MRA [18]. Recently, the relaxation-enhanced angiography without contrast and triggering (REACT) sequence has been introduced as a novel 3D isotropic flow-independent non-CE-MRA technique [19]. The REACT pulse sequence enables the simultaneous delineation of arteries and veins, and has demonstrated encouraging results in imaging of the thoracic vasculature [20–23], extracranial arteries [24–26], abdominal [27] and pelvic vessels [28]. Nevertheless, its performance regarding the depiction of TRAS is unknown.

The aim of this study was to evaluate the performance of REACT for the imaging of the renal allograft vasculature by comparing the detection of TRAS and other vascular findings as well as subjective and objective image quality criteria to 4D CE-MRA at 3 Tesla.

2. Methods

This single-center study was approved by the local institutional review board. Given the retrospective nature of the study, the institutional review board waived the requirement for written informed consent (reference number: 23-1168-retro).

2.1. Patient population

The authors reviewed the institutional image database at a tertiary care university hospital for renal allograft MRA studies between August 2021 and June 2024. Patients were included in the study if they underwent renal transplantation and a standardized MRI protocol for evaluation of pelvic and renal allograft vessels at 3 Tesla, including both REACT and 4D CE-MRA. Exclusion criteria were absence or technical failure of any MRA pulse sequence.

The following data were obtained from medical records or observed during MRI: age, gender, risk factors for atherosclerosis, date and indication of renal transplantation, and date and indication of MRA.

2.2. Magnetic resonance imaging

A commercially available whole body 3 Tesla MRI system (Philips Ingenia, Philips Healthcare, Best, The Netherlands), equipped with a 28-channel body coil without additional modifications, was used. The Philips Ingenia 3.0 T MRI system used in this study is equipped with gradient coils, offering a maximum magnetic gradient strength of 45 millitesla per meter (mT/m). The corresponding slew rate reaches up to 200 T per meter per second (T/m/s). The imaging protocol comprised the following pulse sequences: T_2-weighted turbo spin echo sequences in both coronal and axial plane, REACT, 4D CE-MRA, and T_1-weighted contrast-enhanced gradient-echo sequences with the modified Dixon technique (mDIXON) for fat suppression in both coronal and axial orientations.

For non-CE-MRA, 3D isotropic flow-independent REACT was acquired in the coronal plane from the level of the aortic bifurcation to the level of the common femoral arteries bifurcation. REACT comprises T_2 preparation and inversion recovery (IR) prepulses, which enhance the native blood signal with long T_1 and T_2, followed by a water and fat selective Dixon reconstruction based on a 7-peak fat model (mDIXON XD, Philips Healthcare) [19,29]. Neither respiratory nor ECG-triggering was employed [27]. Parallel imaging using SENSitivity Encoding (SENSE) was used for acceleration of data acquisition [30]. An acceleration factor of 4.5 was employed, resulting in a nominal acquisition time of 2 min and 49 s.

For the contrast enhanced 3D spoiled gradient echo pulse sequence in this study a predominantly T1-weighted contrast enhanced 3D mDIXON pulse sequence with cartesian read out trajectory was used. It employs the modified Dixon method with dual echo times (TE1 = 1.32 ms, TE2 = 2.4 ms) and a short TR (5.8 ms) to separate water and fat signals, enabling robust and homogeneous fat suppression. A flip angle of 15° and RF spoiling enhance T1 weighting. Acquisition included the abdominal aorta from the level of the diaphragm to the level of the common femoral arteries bifurcation. Initially, a native image was acquired as a mask. Subsequently, gadobutrol (Gadovist, Bayer HealthCare Pharmaceuticals, Berlin, Germany; 0.1 ml/kg body weight) was administered via an antecubital vein at a flow rate of 2 ml/s, followed by a 30 ml saline flush. As determined by a bolus tracking sequence, acquisition in coronal plane was initiated upon the arrival of the contrast agent in the abdominal aorta. No ECG-triggering was employed for 4D CE-MRA. Patients were instructed to perform an end-expiratory breath hold during data acquisition. To achieve high spatiotemporal resolution, the acquisition was combined with SENSE (factor 6) and a keyhole technique, whereby 20 % of the central k-space data was acquired in each dynamic (4D TRACK, Philips Healthcare) [31], resulting in a nominal acquisition time of 0:54 min.

Table 1 provides an overview of the imaging parameters of the MRA pulse sequences.

Table 1
Imaging parameters of REACT = relaxation-enhanced angiography without contrast and triggering and 4D CE-MRA = Contrast-enhanced magnetic resonance angiography, FH = feet head, RL = right left, AP = anterior posterior, SENSE = SENSitivity Encoding, IR = inversion recovery, ms = milliseconds, min = minutes.

MRA Technique	REACT	4D CE-MRA
K-space trajectory	Cartesian	Cartesian
Acquisition orientation	coronal	coronal
Acquired voxel size (mm^3)	1.6 × 1.6 × 1.6 mm^3	0.8 × 1.35 × 2.8 mm^3
Reconstructed voxel size (mm^3)	0.78 × 0.78 × 0.80 mm^3	0.620 × 0.620 × 1.4 mm^3
Field of view (FH x RL x AP) (mm^3)	200 × 500 × 130 mm^3	400 × 400 × 140 mm^3
Repetition time (TR) (ms)	4.6 ms	3.8 ms
Echo time (TE, 1/2) (ms)	1.35/2.7 ms	1.08 ms
Flip angle	15°	25°
Subtraction	n/a	CE-native
T_2 preparation (ms)	50 ms; refocusing pulses 4	n/a
IR delay (ms)	58 ms	n/a
Temporal resolution (s)	n/a	1 s
Acceleration factor	SENSE 4.5	SENSE 6
Nominal acquisition time (min)	2:49 min	0:54 min

2.3. Image analysis

Two board-certified radiologists with seven (R1) and eight (R2) years of experience in MRA utilized a commercially available image viewer (DeepUnity Diagnost 1.1.1.1; Dedalus Healthcare Group, Bonn, Germany) to conduct independent reviews of the MRA images during separate sessions and in a randomized order. Both readers were blinded to clinical and patient data and free to modify the window level. To minimize the potential for recall bias, an interval of four weeks was maintained between the evaluation of the REACT and the 4D CE-MRA.

2.3.1. Assessment of transplant renal artery patency

MRA datasets were graded for TRAS using a 1–4 grading scale: Grade 1: no stenosis, grade 2: at least 25 % but less than 50 % stenosis, grade 3: at least 50 % but less than 75 % stenosis, grade 4: at least 75 % stenosis of vessel lumen. In the event of multiple stenoses, the most severe lesion was deemed the diagnostic grade and subjected to further analysis.

2.3.2. Assessment of vascular variants and other vascular findings

Readers were advised to evaluate potential anatomical variants of the graft arteries (supernumerary transplant arteries or early branching), as well as additional vascular findings including arteriovenous fistula and thrombosis. The term “early branching” is defined as the process of renal vessel division, which occurs prior to the vessel’s entry into the renal hilus. [32].

2.3.3. Subjective assessment of image quality

Based on their delineation, the signal intensity, and contrast to adjacent tissue, the readers rated the subjective vessel quality of the MRA datasets using a 5-point Likert scale (1 = non-diagnostic, 2 = pronounced effect on image quality, 3 = moderate effect on image quality, 4 = slight effect on image quality, 5 = no impairment of image quality). Fig. 1 images illustrating the 5-point Likert scales used to evaluate subjective image quality.

The following arterial vessels were analyzed:

1. Abdominal aorta (AA)
2. Transplant renal artery TA)
3. Transplant renal vein (TV)
4. Common iliac artery (CIA)
5. Common iliac vein (CIV)
6. External iliac artery (EIA)
7. External iliac vein (EIV)
8. Internal iliac artery (IIA)
9. Internal iliac vein (IIV)

Furthermore, the overall presence of image artifacts and image noise were rated on a 5-point Likert scale (1: non-diagnostic, 2: pronounced effect on image quality, 3: moderate effect on image quality, 4: slight effect on image quality, and 5: no impairment of image quality).

2.3.4. Assesment of objective image quality

One radiologist with 4 years of experience in MRA (R3) measured apparent contrast-to-noise (aCNR) and apparent signal-to-noise (aSNR) ratios by drawing a region of interest (ROI) in the same position on source images from REACT (water-only) and 4D CE-MRA in the following vessels [25]:

1. Right and left common iliac artery and vein (3 cm distal to the aortic bifurcation).
2. Right and left external iliac artery and vein (3 cm distal to the iliac bifurcation).
3. Transplant artery and vein (1 cm distal to the origin; in cases of supernumerary renal transplant arteries, the largest vessel was used for analysis).

Additionally, a ROI was placed in the adjacent psoas muscle ipsilateral to the respective vessel as a reference standard for background noise.

The aCNR and aSNR were calculated using the following formula [33–36].

$$aCNR = \frac{(SIvessel - SImuscle)}{SD\ of\ SImuscle} \quad aSNR = \frac{SIvessel}{SD\ of\ SImuscle}$$

For each vessel segment, the mean values of the aCNR and aSNR for both sides were calculated and used for further analysis.

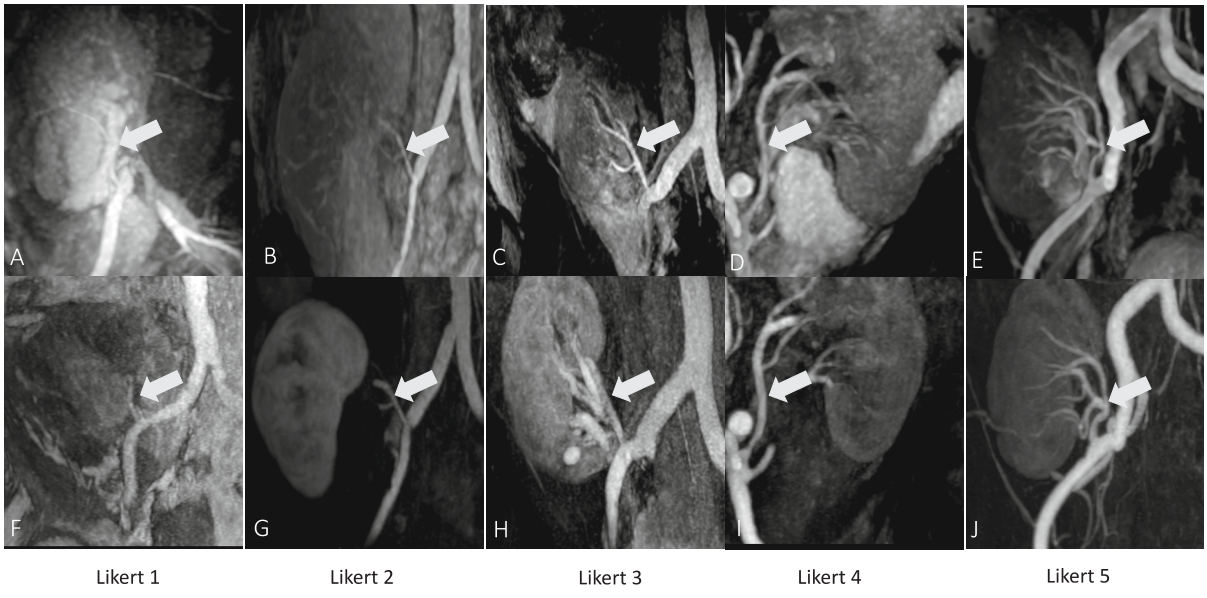

Fig. 1. Maximum intensity projections (MIP, slice thickness 15 mm) with angulation to the hilar region of the transplant kidney. Representative images illustrating the 5-point Likert scales used to evaluate subjective image quality. The transplant renal artery (arrow) was evaluated by the readers for both REACT (A,B,C,D,E) and 4D CE-MRA (F,G,H,I,J) with the following scales: 1 = non-diagnostic, 2 = pronounced effect on image quality, 3 = moderate effect on image quality, 4 = slight effect on image quality, 5 = no impairment of image quality.

2.4. Statistical analysis

Statistical analysis was performed using GraphPad Prism version 10.2.3 for Mac OS X (GraphPad Software). Categorical variables are presented as frequencies and corresponding percentages. Normality distribution of numerical variables was assessed using Shapiro-Wilk tests and visual inspection of Q–Q plots. Normally distributed numerical variables are reported as the mean ± standard deviation (e.g., aSNR, aCNR); otherwise, they are presented as the median and interquartile range (e.g., subjective ratings). To reduce interrater variability and to provide a single representative value per vessel segment and patient for subjective scores, we calculated the mean of the ratings of both readers. Differences between datasets were analyzed using paired *t*-tests for normally distributed data or Wilcoxon signed-rank tests for non-normally distributed data. Spearman's r was calculated to evaluate intersequence and interrater reliability for ranked data such as stenosis grading and subjective ratings. For categorical data, such as vascular findings, Cohen's κ was determined to assess intersequence and interrater agreement. The reliability and strength of agreement for r and κ was interpreted as follows: 0.01–0.20 negligible, 0.21–0.40 weak, 0.41–0.60 moderate, 0.61–0.80 substantial, and 0.81–0.99 almost perfect. Sensitivity and specificity of REACT were calculated to assess diagnostic accuracy, using 4D CE-MRA as the reference standard. For all statistical tests, a two-tailed *p*-value <0.05 was considered statistically significant.

3. Results

3.1. Study population and baseline characteristics

A total of 52 consecutive patients underwent renal allograft vessel imaging with 4D CE-MRA and REACT between August 2021 and June 2024. Five cases were excluded from the study due to the absence of REACT, two cases due to the absence of 4D CE-MRA. Four cases were excluded due to technical failure of 4D CE-MRA, one case was excluded due to technical failure of REACT. None had to be excluded due to motion artifacts. One patient was examined twice. Therefore, the final study population consisted of 40 cases in 39 patients (mean age 48.5 ± 15.1; 14 females). Fig. 2 offers a visual representation of the workflow for the inclusion and exclusion of study participants. Table 2 presents an overview of patient characteristics, renal transplantation, indication for MRA, cardiovascular risk factors and underlying diseases.

3.2. Acquisition time

The total acquisition time of REACT including time needed for image reconstruction was 4:33 [3:58–5:20] minutes, whereas 4D CE-MRA (including the native acquisition and bolus tracking sequence) lasted 3:41 [3:38–4:46] minutes ($p < 0.001$).

3.3. Assessment of transplant artery patency

Overall, 15 TRAS were found in 4D CE-MRA by both readers, of which 10 were considered clinically relevant (≥50 % lumen reduction). Using 4D CE-MRA as the standard of reference, REACT provided a

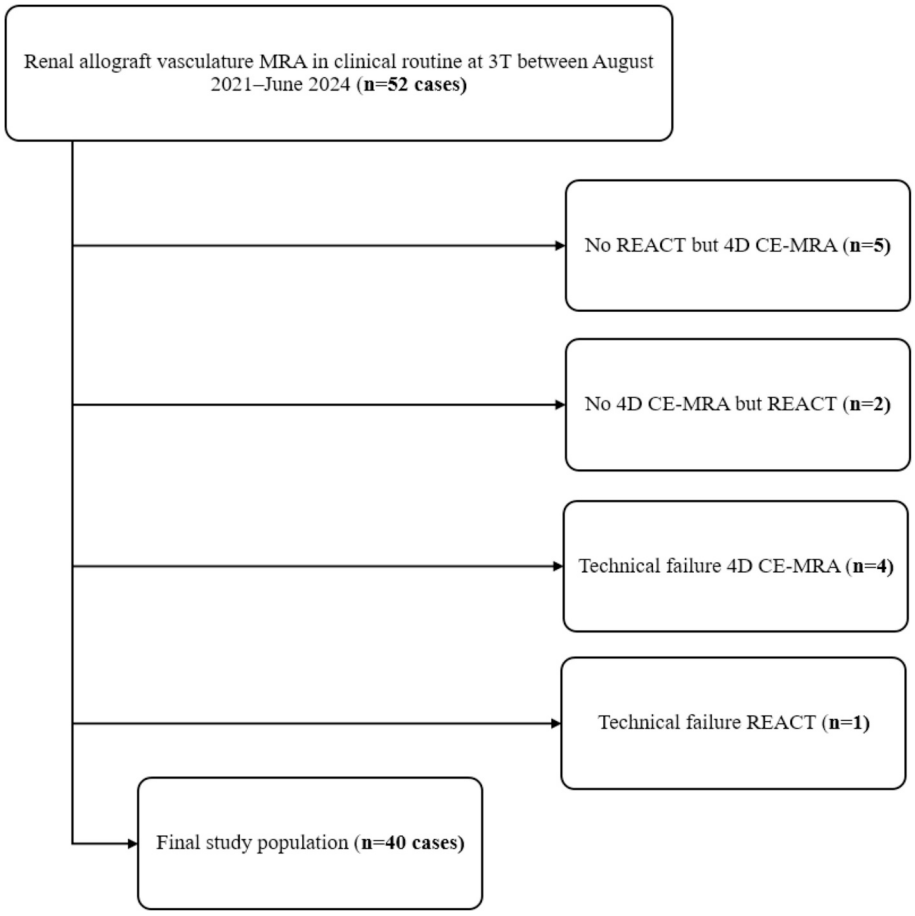

Fig. 2. Workflow for patient inclusion and exclusion. MRA = magnetic resonance angiography, REACT = relaxation-enhanced angiography without contrast and triggering, T = Tesla, 4D CE-MRA = time-resolved contrast-enhanced magnetic resonance angiography.

Table 2
Patient characteristics; BMI=Body mass index, DSA = digital subtraction angiography, GFR = glomerular filtration rate, IgA = immunoglobulin A, MRA = magnetic resonance angiography, ml = millilitre, min = minute, n = number, SD = standard deviation.

Cases, n	40	
Age (years, mean ± SD)	48.5 ± 15.1	
GFR at time of MRA (ml/min, mean ± SD)	38.8 ± 17.2	
Days between surgery and MRA (median [IQR])	42.0 [17–105]	
	n	%
Gender		
Female	14	35.0
Male	26	65.0
Renal transplant		
Living donor	26	65.0
Deceased donor	14	35.0
DSA performed	2	5.0
Indication for MRA		
Transplant renal artery stenosis	24	60.0
Transplant renal artery dissection	3	7.5
Transplant renal artery aneurysm	2	5.0
Transplant renal malfunction	11	27.5
Cardiovascular risk factors		
Arterial hypertension	31	77.5
Diabetes mellitus	2	5.0
Dyslipidemia	11	27.5
Smoking	5	12.5
Underlying disease		
Glomerulonephritis	11	27.5
Ischemic nephropathy	6	15.0
Polycystic kidney disease	5	12.5
Renal vasculitis	4	10.0
Glomerulosclerosis	7	17.5
IgA-nephropathy	4	10.0
Renal amyloidosis	3	7.5

sensitivity of 90.0 % and specificity of 100.0 % for all stenoses and a sensitivity of 90.0 % and specificity of 100.0 % for clinically relevant findings. For stenoses detection both methods had a similar diagnostic confidence (REACT: median 4.0 [4.0–4.0] vs. 4D CE-MRA: 4.0 [3.0–4.0], $p = 0.54$). Regarding stenosis grading, REACT obtained an almost perfect intersequence agreement with 4D CE-MRA ($r = 0.97$). Of note, interrater agreement was perfect in 4D CE-MRA ($r = 1$) and almost perfect in REACT (r = 0.97). Detailed results on stenosis assessment are provided in Table 3.

3.4. Assessment of vascular variants and other vascular findings

Supernumerary renal transplant arteries were the most common vascular variants followed by early branching of the renal transplant artery. Considering 4D CE-MRA as the reference standard, REACT yielded a sensitivity of 93.8 % and specificity of 100.0 % for the delineation of vascular variants. For the detection of other vascular findings (transplant artery thrombosis, $n = 2$; and arterio-venous fistula, $n = 1$), REACT provided a sensitivity of 100.0 % and specificity of 100 %. Combined, REACT obtained a sensitivity of 94.3 % and specificity of 100.0 % for all vascular findings other than stenosis.

Table 3
Stenosis grading for both readers combined in 4D contrast-enhanced magnetic resonance angiography (CE-MRA) and REACT = relaxation-enhanced angiography without contrast and triggering.

	No stenosis	25 % ≤ stenosis < 50 %	50 % ≤ stenosis < 75 %	75 % ≤ stenosis
4D CE-MRA (pooled)	25 (62.5 %)	5 (12.5 %)	4 (10.0 %)	6 (15.0 %)
REACT (pooled)	26.5 (66.25 %)	4.5 (11.25 %)	3 (7.5 %)	6 (15 %)

A detailed summary of vascular variants and other vascular findings is given in Table 4. REACT yielded an excellent intersequence agreement with 4D CE-MRA for the detection of vascular variants and other findings ($\kappa = 0.97$), while the interobserver agreement was excellent in both REACT ($\kappa = 0.97$) and 4D CE-MRA ($\kappa = 1$).

3.5. Assessment of subjective image quality

For all arteries combined, subjective vessel quality was slightly higher in 4D CE-MRA (median 4.0 [IQR: 4.4–4.0.]), although comparable to REACT (4.0 [3.7–4.4]; $p = 0.49$). For all veins combined, subjective image quality was higher in REACT (3.3 [3.0–3.5]) than in 4D CE-MRA (2.4 [2.0–3.0]; $p < 0.001$). Image artifacts and image noise were less pronounced in REACT compared to 4D-MRA (both: $p < 0.001$).

A detailed summary for subjective assessment of image quality, noise, and artifacts is given in Table 5.

3.6. Assesment of objective image quality

For the transplant renal artery, there was no difference regarding aSNR (4D CE-MRA: mean 45.9 ± 21.0 vs. REACT: 44.5 ± 18.2; $p = 0.71$) and aCNR (41.0 ± 20.0 vs. 36.3 ± 15.0; $p = 0.16$) between MRA pulse sequences. Furthermore, aSNR (37.1 ± 19.8 vs. 30.3 ± 15.2; $p = 0.06$) and aCNR (25.0 ± 14.7 vs. 29.4 ± 17.1; $p = 0.17$) did not differ between 4D CE-MRA and REACT at the transplant renal vein. While 4D CE-MRA yielded higher scores for aSNR and aCNR at the CIA and for aCNR at the EIA, REACT demonstrated higher values at the analyzed iliac veins. Table 6 provides detailed aSNR and aCNR results for each imaging modality and segment.

Figs. 3–6 give exemplary comparisons for the depiction of the renal allograft vasculature using REACT and 4D CE-MRA.

4. Discussion

For renal allograft vasculature imaging, a novel 3D isotropic flow-independent MRA technique (REACT) was evaluated for non-contrast imaging at 3 T by comparing the detection of TRAS and other vascular findings as well as subjective and objective image quality criteria to 4D CE-MRA. The main findings of this study are the following: 1. REACT provides comparable results to 4D-CE-MRA in the detection of TRAS, variants and other diagnostic findings. 2. Without gadolinium-based contrast agents or respiratory and cardiac triggering, REACT yields to 4D CE-MRA comparable subjective image quality of the pelvic and renal allograft vessels with equal objective image quality at the transplant vessels.

Previous studies investigating CE-MRA and non-CE-MRA for the assessment of the renal transplant vasculature used DSA as the standard of reference. In a recent meta-analysis including eight CE-MRA studies using either gadolinium- or ferumoxytol-enhanced MRA and three non-CE-MRA studies using primarily SSFP-MRA, Huang et al. reported a pooled sensitivity and specificity of 96 % and 93 % for TRAS [16]. Based on these findings, the authors recommend the routine use of MRA for the diagnosis of TRAS [16]. Given the reported high pooled sensitivity of 89 % and specificity of 94 % for CE-MRA [16], and the fact that only two patients received additional DSA, we chose 4D CE-MRA as the standard of reference in this work. In this regard, REACT obtained a sensitivity of 90 % and a specificity of 100 % for TRAS with equal diagnostic confidence and high intersequence agreement, which is comparable to the pooled sensitivity of 90 % and specificity of 88 % for non-CE-MRA compared to DSA as reported in the above referenced meta-analysis

Table 4
Vascular anomalies and vascular findings for both readers combined. AV = arterio-venous.

	Early branching	Aneurysm	Dissection	Super-numeray artery	AV-fistula	Arterial thrombosis	Venous thrombosis
4D-MRA (pooled)	13 (32.5 %)	0 (0 %)	0 (0 %)	19 (47.5 %)	1 (2.5 %)	2 (5 %)	0 (0 %)
REACT (pooled)	12.5 (31.25 %)	0 (0 %)	0 (0 %)	17.5 (43.75 %)	1 (2.5 %)	2 (5 %)	0 (0 %)

Table 5
Subjective image quality scores of REACT and 4D CE-MRA. To reduce interrater variability and to provide a single representative value per vessel segment and patient for subjective scores, we calculated the mean of the ratings of both readers. The reported values represent the median and interquartile range (IQR) of these averaged scores across all patients. *P*-values were calculated using wilcoxon signed-rank test. Bold indicates statistical significance. AA = abdominal aorta, CIA = common iliac artery, CIV = common iliac vein, 4D CE-MRA = contrast-enhanced magnetic resonance angiography, EIA = external iliac artery, EIV = external iliac vein, IVC = inferior vena cava, IIA = internal iliac artery, IQR = interquartile range, IIV = internal iliac vein, REACT = relaxation-enhanced angiography without contrast and triggering, SD = standard deviation, TA = renal transplant artery, TV = renal transplant vein. Scoring scales of 1–5 were used, 1 being non-diagnostic.

	REACT	4D-MRA	p (wilcoxon)
	median [IQR]	median [IQR]	
Arteries			
AA	4 [3–4.9]	4 [4–5]	0.13
CIA	4 [3.5–4.7]	4.125 [4–4.5]	0.24
EIA	4 [4–4.8]	4 [4–4.5]	0.80
IIA	4 [4–4]	4 [3.5–4.4]	0.66
TA	4 [4–4.5]	4 [4–4]	0.53
All arteries	4 [3.7–4.4]	4 [4–4.4]	0.49
Spearman's r	0.90	0.97	
Veins			
IVC	3 [3–4]	3 [2–3]	**0.005**
CIV	3 [3–3.9]	3 [2–3]	**<0.001**
EIV	3 [3–4]	2.4 [2–3]	**<0.001**
IIV	3 [2.6–3.8]	2 [1.5–3]	**<0.001**
TV	3.5 [3–4]	3 [3–4]	**0.02**
All veins	3.2 [3–3.5]	2.4 [2–3]	**<0.001**
Spearman's r	0.95	0.98	
Noise	4 [3–4]	3 [3–4]	**<0.001**
Spearman's r	0.88	0.93	
Artifacts	4 [4–4.5]	3.3 [3–4]	**<0.001**
Spearman's r	0.85	0.91	

Table 6
Objective image quality pooled for both readers of contrast enhanced MRA compared to REACT. The reported values represent the median and standard deviation of the averaged scores across all patients. P-values were calculated using paired t-test. Bold indicates statistical significance. CIA = common iliac artery, CIV = common iliac vein, 4D CE-MRA = contrast-enhanced magnetic resonance angiography, EIA = external iliac artery, EIV = external iliac vein, IVC = inferior vena cava, IIA = internal iliac artery, IIV = internal iliac vein, REACT = relaxation-enhanced angiography without contrast and triggering, SD = standard deviation, TA = renal transplant artery, TV = renal transplant vein.

	REACT	4D CE-MRA	p (paired t-test)
aSNR (mean ± SD)			
CIA	37.9 ± 13.5	51.8 ± 17.6	**<0.001**
EIA	46.4 ± 16.2	51.2 ± 17.3	0.09
TA	44.5 ± 18.2	45.9 ± 21.0	0.71
CIV	22.4 ± 8.1	11.3 ± 5.0	**<0.001**
EIV	27.4 ± 11.8	11.3 ± 6.3	**<0.001**
TV	37.1 ± 19.8	30.3 ± 15.2	0.06
aCNR (mean ± SD)			
CIA	31.2 ± 12.6	47.6 ± 16.8	**<0.001**
EIA	38.9 ± 14.5	47.5 ± 16.9	**0.002**
TA	36.3 ± 15.0	41.0 ± 20.0	0.16
CIV	16.4 ± 6.9	7.4 ± 4.7	**<0.001**
EIV	20.3 ± 9.9	7.2 ± 5.8	**<0.001**
TV	29.4 ± 17.1	25.0 ± 14.7	0.17

[16]. Of note, an almost perfect intersequence agreement between REACT and 4D CE-MRA ($r = 0.96$) regarding grading of disease as well as an almost perfect interrater agreement in REACT ($r = 0.97$) was observed in the current study, being higher than for QISS-MRA and bSSFP-MRA in a study by Serhal et al., which both showed a moderate interrater agreement ($\kappa = 0.74$ and $\kappa = 0.77$, respectively) [18]. Additionally, the reported findings of the present study are in line with the diagnostic performance of different non-CE-MRA techniques for the detection of stenosis of native renal arteries compared to CE-MRA. For free-breathing inflow IR-bSSFP-MRA compared to CE-MRA, Glockner et al. reported sensitivities of 82–94 % and specificities of 82–86 % at 1.5 T [37] while Lal et al. reported sensitivities of 97–98 % and specificities of 95–98 % at 3 T [38]. For REACT, Gietzen et al. reported an overall sensitivity of 87.5 % and specificity of 100 % for clinically relevant stenosis of the visceral arteries including renal arteries compared to 4D CE-MRA [27].

Regarding the delineation of vascular findings other than stenosis, including supernumerary transplant arteries, transplant artery thrombosis and arterio-venous fistula, REACT obtained a sensitivity of 94.2 % and specificity of 100 %. While above referenced studies solely focused on TRAS, the present study is the first to evaluate these additional findings after renal transplant. Interestingly, almost 50 % of patients harboured supernumerary transplant arteries, due to the fact that the highly specialized transplantation surgery team at the author's institution routinely receive donor kidneys with supernumerary renal arteries. These results align with reported findings for non-CE-MRA techniques in patients with native renal arteries. For REACT, Gietzen et al. reporting a sensitivity of 89.5 % and a specificity of 100 % [27] for the detection of abnormalities of the visceral arteries. For quadruple IR-bSSFP-MRA, Atanasova et al. reported a sensitivity of 75–100 % [40] regarding the delineation of supernumerary renal arteries and renal artery aneurysms [39] while Glockner et al. reported a sensitivity of 93 % and specificity of 100 % for the detection of aberrant renal arteries [37]. For QISS-MRA, Adnersson et al. reported a sensitivity of 86 % and a specificity of 100 % for supernumerary renal arteries in patients prior to living kidney donation [40].

In this work, REACT obtained a subjective image quality at pelvic arteries equal to 4D CE-MRA while providing to 4D CE-MRA superior results regarding the depiction of pelvic veins. These differences are mostly due to the technically demanding acquisition of 4D CE-MRA, especially in patients after surgery with potentially deteriorated general condition, leading to decreased vessel contrast, predominantly affecting venous vessels if the contrast agent has not accumulated in the respective vasculature [15]. In contrast, REACT provides a simultaneous delineation of arteries and veins in a single acquisition over a large field of view [19], being beneficial if both arteries and veins are to be examined, as already demonstrated in various publications regarding the application of REACT for the imaging of the thoracic vasculature [20,22]. These results align in part with the objective image quality evaluation with REACT yielding higher aSNR and aCNR at pelvic veins and the transplant vein, the latter without statistical significance. While

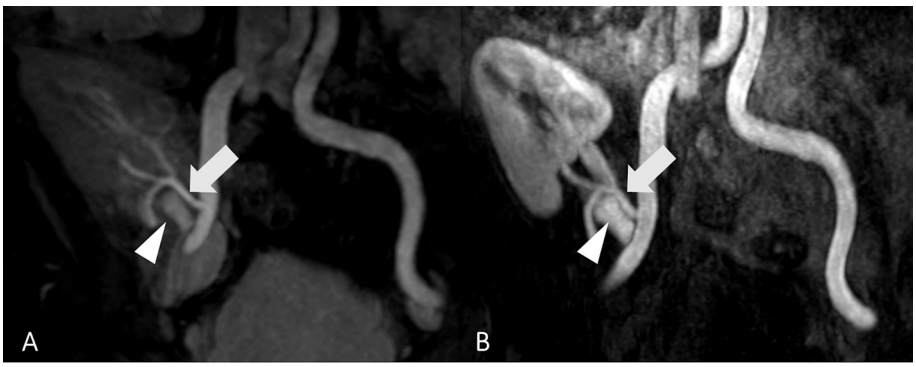

Fig. 3. Maximum intensity projection (MIP, slice thickness 10 mm) with angulation to the hilar region of the transplant kidney in a 19-year-old female patient with suspected transplant renal artery stenosis. Relaxation-enhanced angiography without contrast and triggering (REACT, A) enables a sharper delineation of the transplant kidney artery (arrows) compared to 4D contrast-enhanced magnetic resonance angiography (4D CE-MRA, B) being hampered by venous contamination of the transplant renal vein (arrowheads) and pulsation artifacts.

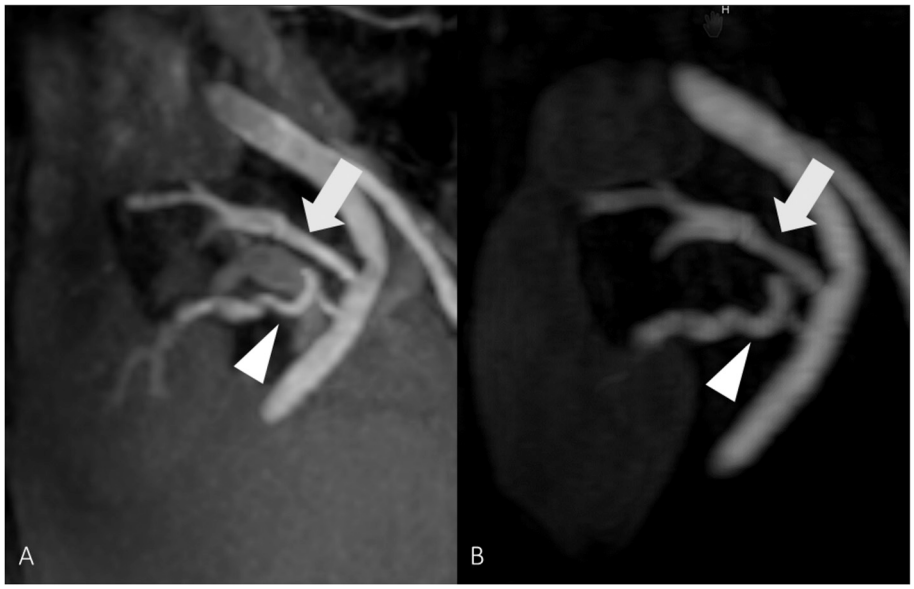

Fig. 4. Maximum intensity projections (MIP, slice thickness 15 mm) in coronar reformation of relaxation-enhanced angiography without contrast and triggering (REACT, A) and 4D contrast-enhanced magnetic resonance angiography (4D CE-MRA, B) in a 23-year-old female patient after renal allograft transplantation and impaired renal function. MRA was performed to rule out TRAS. Both pulse sequences enable the exclusion of TRAS, while depicting a supernumerary renal graft artery (arrowheads) inferior to the main transplant renal artery (arrows).

the objective results at the pelvic arteries are divergent, REACT yielded to 4D CE-MRA equal results for the most important vessel, the transplant artery. Compared to 4D CE-MRA and as demonstrated in numerous studies for the thoracic vasculature [20,22] and carotid arteries [25], REACT was less impaired by artifacts and image noise while 4D CE-MRA was hampered by pulsation artifacts and a higher image noise.

While SSFP-MRA [17] and QISS-MRA [18] as already introduced non-CE-MRA techniques for the depiction of the renal allograft vasculature use ECG-gating during data acquisition, REACT does not require any type of triggering, hence facilitating its use in clinical routine. In contradistinction to the 2D acquisition of QISS-MRA [39], REACT provides a 3D isotropic cartesian readout, thereby enabling post-acquisition reformatting in any arbitrary orientation. This facilitates improved visualization of the complex postoperative vasculature. Furthermore, the mDIXON XD readout provides robust suppression of fat and background and allows for separation of water and fat, consequently leading to insensitivity of inhomogeneities in the magnetic field while SSFP-MRA is highly sensitive to off-resonance effects caused by B_0 heterogeneities and disruptions of the steady state due to highly pulsatile flow or motion and shows high background signals [41,42].

4.1. Limitations

We acknowledge that our retrospective single-centre study has several limitations. Firstly, and as mentioned above, 4D CE-MRA was used as the standard of reference while no comparison to DSA was performed, the latter being the reference standard for visceral artery imaging. Nevertheless, we chose 4D CE-MRA as the standard of reference given the high diagnostic performance of CE-MRA after renal transplant [16] and since only two patients received DSA, hence, a sufficient intraindividual comparison of MRA techniques to DSA was not feasible. However, while arteries yielded the same subjective image quality scores in both MRA sequences, the difference in results regarding the pelvic veins between both MRA must be interpreted with caution due to the lack of a reference standard to confirm these findings. Secondly, we chose to use time resolved 4D CE-MRA as the contrast-enhanced technique. However, it is possible that first-pass 3D CE-MRA would provide a higher spatial resolution and potentially more accurate spatial vascular assessment [43]. Nevertheless, we routinely acquire 4D CE-MRA at our institution, given its additional information depicting the entire pelvic vasculature to detect potential venous pathologies

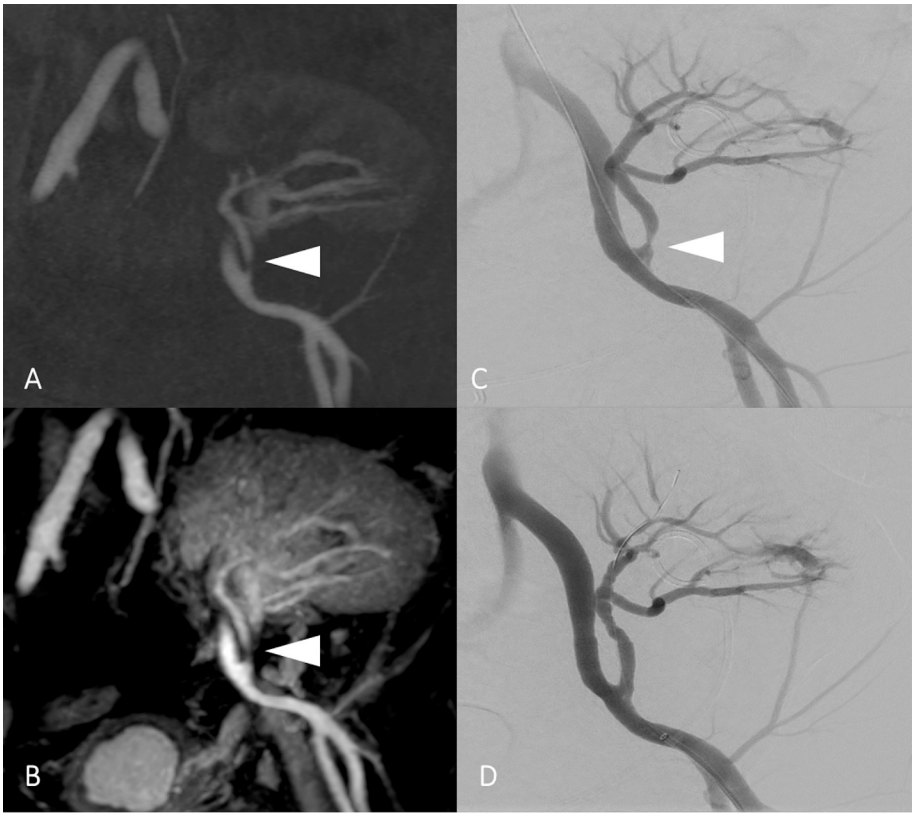

Fig. 5. Maximum intensity projections (MIP, slice thickness: 10 mm) in coronal reformation and angulation to the renal allograft in relaxation-enhanced angiography without contrast and triggering (REACT; A) and 4D contrast-enhanced magnetic resonance angiography (4D CE-MRA; B) in a 67-year-old male patients with anuria. Both MRA sequencec depict a high grade transplant renal artery stenosis with high agreement (arrowhead). In the subsequently performed digital subtraction angiography (DSA), the stenosis was confirmed (C, arrowhead) and treated using percutaneous transluminal angioplasty angioplasty, leading to regular patency of the renal graft artery (D).

which might be missed using first-pass CE-MRA. Of note, the associated potential impact of venous contamination, which might lead to inferior image quality in both 4D CE-MRA and REACT [25], was not evaluated in the present work but may be investigated in future studies when directly comparing different non-CE-MRA techniques for the depiction of the pelvic vasculature with QISS-MRA being routinely not impaired by venous signal [44]. Thirdly, it is possible that the order of acquisition sequences may have an impact on the results of 4D CE-MRA in patients who exhibit motion artifacts towards the conclusion of the examination. Fourthly, the different appearances of 4D CE-MRA and REACT made it impossible to blind the readers to the type of MRA, which may have had an impact on the results. Finally, the selected acceleration technique (parallel imaging using SENSE) and factor for REACT was based on the authors' clinical experience, without a direct comparison of different techniques and undersampling factors. While Compressed SENSE, referring to the combination of parallel imaging and compressed sensing [45], led to a decrease in acquisition time and promising results in imaging of the cervical [24–26,46] and thoracic vasculature [20–22] as well as of the visceral arteries [27], we chose to only use parallel imaging for imaging of the pelvic vessels given the decrease in SNR and CNR when using Compressed SENSE [47]. Nevertheless, the combination of Compressed SENSE with deep learning-based image reconstructions, may be feasible for REACT after renal transplantation [45]. This could result in a reduction of acquisition time while maintaining image quality, which could be a valuable contribution to future research on REACT.

5. Conclusion

In a short acquisition time of less than five minutes, REACT provides high diagnostic performance for identifying TRAS and other vascular findingswhile yielding to to 4D CE-MRA comparable image quality of the pelvic vasculature based on subjective and objective measures. These findings highlight the potential of REACT for imaging of the renal allograft vasculature without the use of gadolinium contrast in patients after renal transplantation.

CRediT authorship contribution statement

Carsten Gietzen: Writing – review & editing, Writing – original draft, Visualization, Validation, Supervision, Resources, Project administration, Methodology, Investigation, Formal analysis, Data curation, Conceptualization. **Juliana Tristram:** Investigation, Data curation. **Jan Paul Janssen:** Investigation, Formal analysis, Data curation. **Marielle Hummels:** Validation, Resources, Formal analysis, Data curation. **Johannes Bremm:** Validation, Resources, Data curation. **Kenan Kaya:** Resources, Data curation. **Thorsten Gietzen:** Validation, Investigation, Data curation. **Henry Pennig:** Validation, Data curation. **Roman Gertz:** Validation, Data curation. **Thorsten Persigehl:** Validation, Supervision, Resources, Project administration, Methodology. **Dirk Stippel:** Validation, Supervision, Resources, Project administration, Methodology, Conceptualization. **Kilian Weiss:** Validation, Software. **Lenhard Pennig:** Writing – review & editing, Writing – original draft, Validation, Supervision, Project administration, Methodology, Investigation, Formal analysis, Conceptualization.

Ethics approval and consent to participate

The local ethics committee approved this study. Due to the retrospective design of the study, written informed consent requirement was

Fig. 6. Maximum intensity projections (MIP, slice thickness: 10 mm) in coronal reformation in relaxation-enhanced angiography without contrast and triggering (REACT, A) and 4D contrast-enhanced magnetic resonance angiography (4D CE-MRA, B) in a 79-year-old male patient referred for graft imaging after diagnostic renal transplant biopsy due to suspected transplant rejection. Both REACT and 4D CE-MRA enable a precise delineation of the early fistula blush (arrowheads), suggesting the presence of an arteriovenous fistula arising from the graft artery (arrow). In the subsequently performed digital subtraction angiography, the AV-fistula was successfully sealed in its entirety (C and D).

waived.

Ethics comittee: Ethikkommission, Medizinische Fakultät der Universität zu Köln.

Committee's reference number: 23–1168.

Funding

None.

Declaration of competing interest

Roman Johannes Gertz: Speaker's bureau, Philips Healthcare. Speakers' bureau, Guerbet GmbH.

David Maintz: Speaker's bureau, Philips Healthcare.

Kilian Weiss: Employee, Philips Healthcare.

Lenhard Pennig: Speaker's bureau, Philips Healthcare. Speakers' bureau, Guerbet GmbH.

The other authors have no conflicts of interest to declare.

Acknowledgements

Clinician Scientist position supported by the Deans Office, Faculty of Medicine, University of Cologne.

Data availability

The datasets generated and/or analyzed during the current study are not publicly available due to data protection but are available from the corresponding author upon reasonable request.

The imaging protocol of the proposed REACT sequence is available from the corresponding author upon reasonable request.

References

[1] Wey A, Gustafson SK, Salkowski N, et al. Program-specific transplant rate ratios: association with allocation priority at listing and posttransplant outcomes. Am J Transplant 2018;18:1360–9. https://doi.org/10.1111/ajt.14684.

[2] World Health Organization. International Report on Organ Donation and Transplantation Activities, Executive Summary. Geneva: World Health Organization; 2023.

[3] Seratnahaei A, Shah A, Bodiwala K, Mukherjee D. Management of Transplant Renal Artery Stenosis. Angiology 2011;62:219–24. https://doi.org/10.1177/0003319710377076.

[4] Robinson KA, Kriegshauser JS, Dahiya N, et al. Detection of transplant renal artery stenosis: determining normal velocities at the renal artery anastomosis. Abdominal Radiology 2017;42:254–9. https://doi.org/10.1007/s00261-016-0876-7.

[5] Patel NH, Jindal RM, Wilkin T, et al. Renal arterial stenosis in renal allografts: retrospective study of predisposing factors and outcome after percutaneous transluminal angioplasty. Radiology 2001;219:663–7. https://doi.org/10.1148/radiology.219.3.r01jn30663.

[6] Sugi MD, Joshi G, Maddu KK, et al. Imaging of renal transplant complications throughout the life of the allograft: comprehensive multimodality review. RadioGraphics 2019;39:1327–55. https://doi.org/10.1148/rg.2019190096.

[7] de Morais RH, Muglia VF, Mamere AE, et al. Duplex Doppler sonography of transplant renal artery stenosis. J Clin Ultrasound 2003;31:135–41. https://doi.org/10.1002/jcu.10147.

[8] Ismaeel MM, Abdel-Hamid A. Role of high resolution contrast-enhanced magnetic resonance angiography (HR CeMRA) in management of arterial complications of the renal transplant. Eur J Radiol 2011;79:e122–7. https://doi.org/10.1016/j.ejrad.2011.04.039.

[9] Fananapazir G, Bashir MR, Corwin MT, et al. Comparison of ferumoxytol-enhanced MRA with conventional angiography for assessment of severity of transplant renal artery stenosis. J Magn Reson Imaging 2017;45:779–85. https://doi.org/10.1002/jmri.25421.

[10] Wilkinson A. Protocol transplant biopsies. Clin J Am Soc Nephrol 2006;1:130–7. https://doi.org/10.2215/CJN.00350705.

[11] Weinreb JC, Rodby RA, Yee J, et al. Use of intravenous gadolinium-based contrast Media in Patients with kidney disease: consensus statements from the American College of Radiology and the National Kidney Foundation. Radiology 2021;298:28–35. https://doi.org/10.1148/radiol.2020202903.

[12] Perazella MA. Advanced kidney disease, gadolinium and nephrogenic systemic fibrosis: the perfect storm. Curr Opin Nephrol Hypertens 2009;18:519–25. https://doi.org/10.1097/MNH.0b013e3283309660.

[13] Gulani V, Calamante F, Shellock FG, et al. Gadolinium deposition in the brain: summary of evidence and recommendations. Lancet Neurol 2017;16:564–70. https://doi.org/10.1016/S1474-4422(17)30158-8.

[14] Jung J-W, Kang H-R, Kim M-H, et al. Immediate hypersensitivity reaction to gadolinium-based MR contrast media. Radiology 2012;264:414–22. https://doi.org/10.1148/radiol.12112025.

[15] Menke J. Carotid MR angiography with traditional bolus timing: clinical observations and Fourier-based modelling of contrast kinetics. Eur Radiol 2009;19:2654–62. https://doi.org/10.1007/s00330-009-1448-9.

[16] Huang Y, Zhang B, Zheng J, et al. Diagnostic performance of magnetic resonance angiography for artery stenosis after kidney transplant: a systematic review and meta-analysis. Acad Radiol 2023;30:2021–30. https://doi.org/10.1016/j.acra.2023.02.034.

[17] Lanzman RS, Voiculescu A, Walther C, et al. ECG-gated nonenhanced 3D steady-state free precession MR angiography in assessment of transplant renal arteries: comparison with DSA. Radiology 2009;252:914–21. https://doi.org/10.1148/radiol.2531082260.

[18] Serhal A, Aouad P, Serhal M, et al. Evaluation of renal allograft vasculature using non-contrast 3D inversion recovery balanced steady-state free precession MRA and 2D quiescent-interval slice-selective MRA. Explor Res Hypothesis Med 2021;000:000. https://doi.org/10.14218/ERHM.2021.00011.

[19] Yoneyama M, Zhang S, Hu HH, et al. Free-breathing non-contrast-enhanced flow-independent MR angiography using magnetization-prepared 3D non-balanced dual-echo Dixon method: a feasibility study at 3 tesla. Magn Reson Imaging 2019;63:137–46. https://doi.org/10.1016/j.mri.2019.08.017.

[20] Pennig L, Wagner A, Weiss K, et al. Imaging of the pulmonary vasculature in congenital heart disease without gadolinium contrast: Intraindividual comparison of a novel compressed SENSE accelerated 3D modified REACT with 4D contrast-enhanced magnetic resonance angiography. J Cardiovasc Magn Reson 2020;22:8. https://doi.org/10.1186/s12968-019-0591-y.

[21] Gietzen C, Pennig L, von Stein J, et al. Thoracic aorta diameters in Marfan patients: Intraindividual comparison of 3D modified relaxation-enhanced angiography without contrast and triggering (REACT) with transthoracic echocardiography. Int J Cardiol 2023;390:131203. https://doi.org/10.1016/j.ijcard.2023.131203.

[22] Pennig L, Wagner A, Weiss K, et al. Comparison of a novel compressed SENSE accelerated 3D modified relaxation-enhanced angiography without contrast and triggering with CE-MRA in imaging of the thoracic aorta. Int J Cardiovasc Imaging 2021;37:315–29. https://doi.org/10.1007/s10554-020-01979-2.

[23] Betz LH, Dillman JR, Towbin AJ, et al. Respiratory-triggered flow-independent noncontrast non–ECG-gated MRV (REACT) versus CE-MRV for central venous evaluation in children and Young adults: a six-reader study. Am J Roentgenol 2023;221:240–8. https://doi.org/10.2214/AJR.22.28893.

[24] Hoyer UCI, Lennartz S, Abdullayev N, et al. Imaging of the extracranial internal carotid artery in acute ischemic stroke: assessment of stenosis, plaques, and image quality using relaxation-enhanced angiography without contrast and triggering (REACT). Quant Imaging Med Surg 2022;12:3640–54. https://doi.org/10.21037/QIMS-21-1122/COIF).

[25] Pennig L, Kabbasch C, Hoyer UCI, et al. Relaxation-enhanced angiography without contrast and triggering (REACT) for fast imaging of extracranial arteries in acute ischemic stroke at 3 T. Clin Neuroradiol 2021;31:815–26. https://doi.org/10.1007/s00062-020-00963-6.

[26] Gietzen C, Kaya K, Janssen JP, et al. Highly compressed SENSE accelerated relaxation-enhanced angiography without contrast and triggering (REACT) for fast non-contrast enhanced magnetic resonance angiography of the neck: clinical evaluation in patients with acute ischemic stroke at 3 tesla. Magn Reson Imaging 2024. https://doi.org/10.1016/j.mri.2024.04.009.

[27] Gietzen C, Janssen JP, Görtz L, et al. Non-contrast-enhanced MR-angiography of the abdominal arteries: intraindividual comparison between relaxation-enhanced angiography without contrast and triggering (REACT) and 4D contrast-enhanced MR-angiography. Abdom Radiol (NY) 2024. https://doi.org/10.1007/s00261-024-04639-4.

[28] Terwolbeck MN, Zhang S, Bode M, et al. Relaxation-enhanced angiography without contrast and triggering (REACT) for pelvic MR venography in comparison to balanced gradient-echo and T2-weighted spin-echo techniques. Clin Imaging 2021;74:149–55. https://doi.org/10.1016/j.clinimag.2020.12.029.

[29] Eggers H, Brendel B, Duijndam A, Herigault G. Dual-echo Dixon imaging with flexible choice of echo times. Magn Reson Med 2011;65:96–107. https://doi.org/10.1002/MRM.22578.

[30] Pruessmann KP, Weiger M, Scheidegger MB, Boesiger P. SENSE: sensitivity encoding for fast MRI. Magn Reson Med 1999;42:952–62.

[31] Willinek WA, Hadizadeh DR, von Falkenhausen M, et al. 4D time-resolved MR angiography with keyhole (4D-TRAK): more than 60 times accelerated MRA using a combination of CENTRA, keyhole, and SENSE at 3.0T. J Magn Reson Imaging 2008;27:1455–60. https://doi.org/10.1002/jmri.21354.

[32] Satyapal KS, Haffejee AA, Singh B, et al. Additional renal arteries incidence and morphometry. Surg Radiol Anat 2001;23:33–8. https://doi.org/10.1007/s00276-001-0033-y.

[33] Edelstein WA, Glover GH, Hardy CJ, Redington RW. The intrinsic signal-to-noise ratio in NMR imaging. Magn Reson Med 1986;3:604–18. https://doi.org/10.1002/mrm.1910030413.

[34] Constable RT, Smith RC, Gore JC. Signal-to-noise and contrast in fast spin Echo (FSE) and inversion recovery FSE imaging. J Comput Assist Tomogr 1992;16:41–7. https://doi.org/10.1097/00004728-199201000-00008.

[35] Reeder SB. Measurement of signal-to-noise ratio and parallel imaging. In: Parallel imaging in clinical MR applications. Berlin, Heidelberg: Springer Berlin Heidelberg; 2007. p. 49–61.

[36] Young IR. MRI theory*. In: Encyclopedia of Spectroscopy and Spectrometry. Elsevier; 1999. p. 1638–45.

[37] Glockner JF, Takahashi N, Kawashima A, et al. Non-contrast renal artery MRA using an inflow inversion recovery steady state free precession technique (Inhance): comparison with 3D contrast-enhanced MRA. J Magn Reson Imaging 2010;31:1411–8. https://doi.org/10.1002/jmri.22194.

[38] Lal H, Kunti R, Singh R, et al. Non-contrast MR angiography versus contrast enhanced MR angiography for detection of renal artery stenosis: a comparative analysis in 400 renal arteries. Abdominal Radiology 2021;46:2064–71. https://doi.org/10.1007/s00261-020-02836-5.

[39] Atanasova IP, Lim RP, Chandarana H, et al. Quadruple inversion-recovery b-SSFP MRA of the abdomen: initial clinical validation. Eur J Radiol 2014;83:1612–9. https://doi.org/10.1016/j.ejrad.2014.05.026.

[40] Andersson J, Meik R, Pravdivtseva M, et al. Preoperatively determining renal perfusion and visualizing renal arteries and any abnormalities in potential living kidney donors using non-contrast-enhanced magnetic resonance imaging techniques at 1.5 Tesla. Clin Kidney J 2024. https://doi.org/10.1093/ckj/sfae101.

[41] Bangerter NK, Cukur T, Hargreaves BA, et al. Three-dimensional fluid-suppressed T2-prep flow-independent peripheral angiography using balanced SSFP. Magn Reson Imaging 2011;29:1119–24. https://doi.org/10.1016/j.mri.2011.04.007.

[42] Çukur T, Lee JH, Bangerter NK, et al. Non-contrast-enhanced flow-independent peripheral MR angiography with balanced SSFP. Magn Reson Med 2009;61:1533–9. https://doi.org/10.1002/mrm.21921.

[43] Vogt FM, Theysohn JM, Michna D, et al. Contrast-enhanced time-resolved 4D MRA of congenital heart and vessel anomalies: image quality and diagnostic value compared with 3D MRA. Eur Radiol 2013;23:2392–404. https://doi.org/10.1007/s00330-013-2845-7.

[44] Peters S, Huhndorf M, Jensen-Kondering U, et al. Non-contrast-enhanced carotid MRA: clinical evaluation of a novel ungated radial quiescent-interval slice-selective MRA at 1.5T. Am J Neuroradiol 2019. https://doi.org/10.3174/ajnr.A6171.

[45] Liang D, Liu B, Wang J, Ying L. Accelerating SENSE using compressed sensing. Magn Reson Med 2009;62:1574–84. https://doi.org/10.1002/mrm.22161.

[46] Janssen JP, Rose S, Kaya K, et al. Non-contrast-enhanced MR-angiography of extracranial arteries in acute ischemic stroke at 1.5 Tesla using relaxation-enhanced angiography without contrast and triggering (REACT). Clin Neuroradiol 2024. https://doi.org/10.1007/s00062-024-01458-4.

[47] Bratke G, Rau R, Weiss K, et al. Accelerated MRI of the lumbar spine using compressed sensing: quality and efficiency. J Magn Reson Imaging 2019;49:e164–75. https://doi.org/10.1002/JMRI.26526.